536.423::532.582

Paper No. 214-10

Forced Convection Film Boiling Heat Transfer from a Horizontal Cylinder to Liquid Cross-flowing Upward*

(2nd Report, Subcooled Liquid)

By Tooru SHIGECHI**, Takehiro ITO***

and Kaneyasu NISHIKAWA***

Forced convection film boiling heat transfer from a horizontal cylinder to a subcooled liquid cross-flowing upward is analysed based on the two-phase boundary-layer theory. Numerical solution of the conservation equations is determined for subcooled water, ethanol and hexane under the atmospheric pressure by the method similar to that of the first report for saturated liquid.

The velocity profile, the separation point in the vapor film, the thickness of the boundary-layer and the average Nusselt number are discussed in the same manner as in the previous report and the effects of the subcooling and the approaching velocity on them are also examined. The calculated results on heat transfer are compared with the experimental data.

Key Words: Phase Change, Forced Convection Film Boiling Heat Transfer, Horizontal Cylinder, Subcooled Liquid, Numerical Analysis

1. Introduction

In the first report[1], the forced convection film boiling heat transfer from a horizontal cylinder to a saturated liquid cross-flowing upward was analysed based on the two-phase boundary-layer theory by means of the integral method of boundary-layer.

Motte-Bromley[2] and recently Epstein-Hauser[3] studied the cross-flow forced convection film boiling heat transfer from a horizontal cylinder to a subcooled liquid. In the former, the analysis for a saturated liquid is extended to that for a subcooled liquid to obtain a correlating equation of heat transfer. In the analysis bold assumptions including a one dimensional flow model are adopted. However, their correlation does not seem to fit their own data very well. In the latter, it is assumed that the angular variation of the vapor film thickness is small in the case of a subcooled liquid and that heat transfer over the entire surface is governed by that at the forward stagnation point. A correlating equation of heat transfer is also proposed by interpolating the two limiting cases of large subcooling and small subcooling (including saturated liquid) for pure forced convection film boiling heat transfer from a sphere and a horizontal cylinder. However, the experimental data by Motte-Bromley[2] and others are about twice as large as those given by the correlating equation and a scattering of the data does not disappear though some corrections were made to the original correlating equation derived by their analysis.

In this report, the previous analysis[1] for a saturated liquid is extended to that for a subcooled liquid. Numerical solutions are determined for water, ethanol and hexane under the standard atmospheric pressure. The characteristics of solutions are discussed in the same manner as in the first report and the effect of subcooling is examined. The present analysis is also compared with the semi-theoretical equation by Epstein-Hauser[3] and the experimental data at the atmospheric pressure for ethanol by Motte-Bromley[2] and for water by the present authors[4].

2. Nomenclature

B_L: dimensionless parameter for buoyant force, Eq.(12)
Sc: dimensionless subcooling, Eq.(11)
T_∞: bulk temperature of liquid
ΔT_{sat}: degree of superheating $\equiv T_w - T_s$
ΔT_{sub}: degree of subcooling $\equiv T_s - T_\infty$
β: volumetric coefficient of thermal expansion
Δ_ℓ: dimensionless thickness of liquid boundary-layer (Δ in the first report)
Δ_t: dimensionless thickness of liquid thermal boundary-layer
θ: dimensionless temperature of liquid, Eq.(10)

Subscripts
Δ_ℓ: outer edge of liquid boundary-layer

* Received 27th September, 1980.
** Lecturer, Faculty of Engineering, Nagasaki University, Nagasaki.
*** Professor, Faculty of Engineering, Kyushu University, Fukuoka.

Δt: outer edge of liquid thermal boundary-layer

The other symbols are the same as those in the first report.

3. Fundamental Equations

Consider the film boiling heat transfer from a cylinder with uniform surface temperature T_W, which is placed horizontally in a stream of liquid flowing upward with uniform velocity U_∞ (Fig. 1). The gravitational force g acts in a direction entirely opposite to the approaching velocity of liquid U_∞. The liquid is subcooled by ΔT_{sub} below the saturation temperature T_S corresponding to the system pressure. In deriving the fundamental equations, the same assumptions are employed as those in the first report for a saturated liquid(1). The same equations as in the first report are omitted and the equations modified or enlarged for the presence of liquid subcooling are given below.

As for the vapor film, continuity equation and momentum equation remain unaltered, while energy equations are expressed as follows by introducing a term of heat conduction.

$$y_1=\delta_1 : -\lambda_V\left(\frac{\partial T_V}{\partial y_1}\right)_{\delta_1}=-\dot{m}l-\lambda_L\left(\frac{\partial T_L}{\partial y_1}\right)_{\delta_1} \quad \cdots\cdots(1)$$

$$l\rho_V\frac{1}{r}\frac{d}{d\varphi}\int_0^{\delta_1}u_{V1}dy_1=\frac{\lambda_V(T_W-T_S)}{\delta_1}+\lambda_L\left(\frac{\partial T_L}{\partial y_1}\right)_{\delta_1} \quad \cdots\cdots(2)$$

As for the liquid boundary-layer, a term of buoyant force is added to the momentum equation and furthermore the energy equation itself is incorporated into a set of governing equations.

$$\frac{u_{L_1}}{r}\frac{\partial u_{L_1}}{\partial\varphi}+v_{L_1}\frac{\partial u_{L_1}}{\partial y_1}=g\beta_L(T_L-T_\infty)\sin\varphi+\frac{2U_\infty^2}{r}\sin 2\varphi+\nu_L\frac{\partial^2 u_{L_1}}{\partial y_1^2} \quad \cdots\cdots(3)$$

$$c_{pL}\rho_L\frac{u_{L_1}}{r}\frac{\partial T_L}{\partial\varphi}+c_{pL}\rho_L v_{L_1}\frac{\partial T_L}{\partial y_1}=\lambda_L\frac{\partial^2 T_L}{\partial y_1^2} \quad \cdots\cdots(4)$$

In addition, Eq.(5) as the compatibility condition at the vapor-liquid interface and Eqs.(6) and (7) as the boundary conditions are established to complete the description concerning the liquid thermal boundary-layer.

$$y_1=\delta_1 : T_L=T_S \quad \cdots\cdots(5)$$

$$y_1=\delta_1+\Delta_{t_1} : T_L=T_\infty \quad \cdots\cdots(6)$$

$$\lambda_L\left(\frac{\partial T_L}{\partial y_1}\right)_{\Delta_{t_1}}=0 \quad \cdots\cdots(7)$$

Now, using the dimensionless variables and parameters defined by Eqs. (8) through (12) and (18)* (the number of equation with asterisk means that the equation appears in the first report hereinafter) through (28)*, the fundamental equations, the boundary conditions and the compatibility conditions at the vapor-liquid interface are expressed in dimensionless form as follows.

$$\Delta_l\equiv\Delta_{l_1}(g/\nu_V^2 r)^{1/4} \quad \cdots\cdots(8)$$

$$\Delta_t\equiv\Delta_{t_1}(g/\nu_V^2 r)^{1/4} \quad \cdots\cdots(9)$$

$$\theta\equiv c_{pL}(T_L-T_\infty)/P_{rL}l \quad \cdots\cdots(10)$$

$$S_c\equiv c_{pL}(T_S-T_\infty)/P_{rL}l \quad \cdots\cdots(11)$$

$$B_L\equiv\beta_L l/c_{pL} \quad \cdots\cdots(12)$$

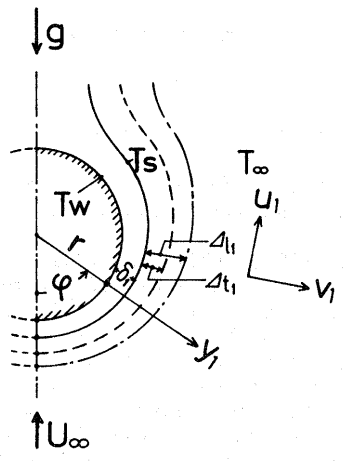

Fig.1 Physical model and co-ordinate system

The energy equation for the vapor film:

$$\delta\frac{d}{d\varphi}\int_0^\delta u_V dy=S_p+\frac{\delta}{R^2K}\left(\frac{\partial\theta}{\partial y}\right)_\delta \quad \cdots\cdots(13)$$

The momentum equation and the energy equation for the liquid boundary-layer:

$$u_L\frac{\partial u_L}{\partial\varphi}+v_L\frac{\partial u_L}{\partial y}=P_{rL}B_L\theta\sin\varphi+\left(\frac{1}{RK}\right)^2\frac{\partial^2 u_L}{\partial y^2}+2f\sin 2\varphi \quad \cdots\cdots(14)$$

$$u_L\frac{\partial\theta}{\partial\varphi}+v_L\frac{\partial\theta}{\partial y}=\frac{1}{P_{rL}}\left(\frac{1}{RK}\right)^2\frac{\partial^2\theta}{\partial y^2} \quad \cdots\cdots(15)$$

The boundary conditions and the compatibility conditions at the vapor-liquid interface:

$$y=\delta : \theta_\delta=S_c \quad \cdots\cdots(16)$$

$$y=\delta+\Delta_t : \theta_{\Delta t}=0 \quad \cdots\cdots(17)$$

$$\left(\frac{\partial\theta}{\partial y}\right)_{\Delta t}=0 \quad \cdots\cdots(18)$$

As for the boundary conditions of the liquid boundary-layer, Δ in Eqs.(38)* and (39)* should be replaced by Δ_l. By incorporating Eqs.(16)* and (13), Eq.(37)* is written as follows

$$\left(v_V-u_V\frac{d\delta}{d\varphi}\right)_\delta=-\frac{S_p}{\delta}-\frac{1}{R^2K}\left(\frac{\partial\theta}{\partial y}\right)_\delta . \quad \cdots\cdots(19)$$

Now, the problem of analysis reduces to finding a solution of the resulting equations, Eqs.(29)*, (30)*, (13), (32)*, (14) and (15), subject to the conditions Eqs.(34)* through (39)* and Eqs.(16) through (18) for seven prescribed parameters, i.e., B_L (buoyant force parameter), Fr (Froude number), K (density ratio), Pr_L (Prandtl number of liquid), R ($\rho\mu$ ratio), Sc (dimensionless subcooling), and Sp (dimensionless superheating). Heat transfer characteristics are calculated in exactly the same manner as in the first report.

4. Method of Solution

We first determine u_V by the method similar to that in the first report. Next, we assume quadratic functions of y for u_L and θ and determine the coefficients of these functions by Eqs.(35)*, (38)* and (39)* for u_L and by Eqs.(16), (17) and (18) for θ .

$$u_L=u_\delta+(2f^{1/2}\sin\varphi-u_\delta)\{(2\zeta/\Delta_t)-(\zeta/\Delta_t)^2\} \quad \cdots\cdots(20)$$
$$\theta=S_c\{1-(\zeta/\Delta_t)\}^2 \quad \cdots\cdots(21)$$

where ζ is defined by Eq.(49)*.

Now, the method of integration of the fundamental equations for the liquid boundary-layer depends on the ratio of the hydrodynamic to thermal boundary-layer thickness, $\Delta\ell/\Delta t$. Here the method of integration is presented only for the case of $\Delta\ell>\Delta t$.

Integrating Eqs.(32)* and (14) from δ to $\delta+\Delta\ell$ with respect to y , we have

$$\frac{d}{d\varphi}\int_\delta^{\delta+\Delta_t}u_L dy-u_{L\Delta_t}\frac{d(\delta+\Delta_t)}{d\varphi}+u_{L\delta}\frac{d\delta}{d\varphi}+(v_{L\Delta_t}-v_{L\delta})=0 \quad \cdots\cdots(22)$$

$$\frac{d}{d\varphi}\int_\delta^{\delta+\Delta_t}u_L^2dy-u_{L\Delta_t}^2\frac{d(\delta+\Delta_t)}{d\varphi}+u_{L\delta}^2\frac{d\delta}{d\varphi}+(v_{L\Delta_t}u_{L\Delta_t}-v_{L\delta}u_{L\delta})$$
$$=Pr_LB_L\sin\varphi\int_\delta^{\delta+\Delta_t}\theta dy-\left(\frac{1}{RK}\right)^2\left(\frac{\partial u_L}{\partial y}\right)_\delta+2f\Delta_t\sin2\varphi. \quad \cdots\cdots(23)$$

Eliminating $v_{L\Delta\ell}$ between Eqs.(22) and (23) and transforming y to ζ , we obtain

$$\frac{d}{d\varphi}\int_0^{\Delta_t}u_L^2d\zeta-u_{L\Delta_t}\frac{d}{d\varphi}\int_0^{\Delta_t}u_Ld\zeta+(u_{L\delta}-u_{L\Delta_t})\left\{\frac{S_p}{K\delta}+\left(\frac{1}{RK}\right)^2\left(\frac{\partial\theta}{\partial\zeta}\right)_0\right\}$$
$$-Pr_LB_L\sin\varphi\int_0^{\Delta_t}\theta d\zeta+\left(\frac{1}{RK}\right)^2\left(\frac{\partial u_L}{\partial\zeta}\right)_0-2f\Delta_t\sin2\varphi=0. \quad \cdots\cdots(24)$$

Integration of Eq.(15) from δ to $\delta+\Delta t$ with respect to y yields

$$\frac{d}{d\varphi}\int_\delta^{\delta+\Delta_t}u_L\theta dy-S_c\left(v_{L\delta}-u_{L\delta}\frac{d\delta}{d\varphi}\right)=-\left(\frac{1}{Pr_L}\right)\left(\frac{1}{RK}\right)^2\left(\frac{\partial\theta}{\partial y}\right)_\delta . \quad \cdots\cdots(25)$$

Substituting Eq.(19) into the above equation and transforming y to ζ , we obtain

$$\frac{d}{d\varphi}\int_0^{\Delta_t}u_L\theta d\zeta+\frac{S_cS_p}{K\delta}+\left(S_c+\frac{1}{Pr_L}\right)\left(\frac{1}{RK}\right)^2\left(\frac{\partial\theta}{\partial\zeta}\right)_0=0. \quad \cdots\cdots(26)$$

We get the relation between δ and $\Delta\ell$ by Eq.(36)* as

$$\Delta_t=\frac{4}{R^2K}\frac{2f^{1/2}\sin\varphi-u_\delta}{2u_\delta-\delta^2K(1+4f\cos\varphi)\sin\varphi}\delta . \quad \cdots\cdots(27)$$

Substituting Eq.(47)* for u_V into Eq.(13) and Eq.(20) for u_L and Eq.(21) for θ into Eq.(24) and Eq.(26) and eliminating $\Delta\ell$ by Eq.(27), we finally obtain the following simultaneous ordinary differential equations for δ , u_δ and Δt.

$$\begin{cases} F_1\dfrac{d\delta}{d\varphi}+F_2\dfrac{du_\delta}{d\varphi}=F_3 & \cdots\cdots(28)\\ F_4\dfrac{d\delta}{d\varphi}+F_5\dfrac{du_\delta}{d\varphi}=F_6 & \cdots\cdots(29)\\ F_7\dfrac{d\delta}{d\varphi}+F_8\dfrac{du_\delta}{d\varphi}+F_9\dfrac{d\Delta_t}{d\varphi}=F_{10} & \cdots\cdots(30)\end{cases}$$

where F_1, F_2, $\cdots$ F_{10} are functions of the variables δ , u_δ, Δt and φ , and the parameters, B_L , Fr , K , Pr_L , R , Sp and Sc . The algebraic expressions of these functions are not given here because of the limitation of space.

Since the simultaneous differential equations, Eqs.(28), (29) and (30), are singular at $\varphi=0$, a forward-integration of them with the conditions of symmetry, i.e., $u_{\delta\varphi=0}=0$, $(d\delta/d\varphi)_{\varphi=0}=0$ and $(d\Delta t/d\varphi)_{\varphi=0}=0$ cannot be directly performed starting there. To overcome this difficulty we expand δ , u_δ and Δt such that $\delta=a_0+a_2\varphi^2$, $u_\delta=b_1\varphi$ and $\Delta t=c_0+c_2\varphi^2$ in the vicinity of $\varphi=0$, and substitute them into Eqs.(28), (29) and (30). By solving the resulting equations the coefficients a_0, a_2, b_1, c_0 and c_2 are determined. These solutions were employed up to 0.1 or 0.2 rad. Starting from this point, Eqs.(28), (29) and (30) were forward integrated by means of Runge-Kutta-Gill method. The numerical integration can be performed up to the rear stagnation point when $Fr\leqq 1/8$. In this case the separation of velocity distribution does not occur in the vapor film for a subcooled liquid as it was the case for a saturated liquid. However, if Fr is larger than 1/8 in the case of a subcooled liquid, the velocity profile in the liquid may become flat

in the upstream region of the separation point φ_{SV} of the velocity distribution in the vapor film (described later in Fig.3 in detail). The magnitude of the tangential velocity in the liquid is equal to that of a free stream everywhere in this situation. This did not occur in the case of a saturated liquid. At this point (designated as φ_{SL}) the boundary-layer thickness of liquid $\Delta\ell$ becomes infinite.

The numerical integration was further performed in the downstream region of the point φ_{SL} assuming that the velocity in the liquid boundary-layer u_L was equal to that of the free stream which was assumed as a potential flow, i.e., $2f^{1/2}\sin\varphi$. When the vapor boundary-layer is going to separate, the scheme of the numerical integration breaks down again (this point is designated as φ_{SV}). In the region downstream of this point, the vapor film thickness δ is arbitrarily assigned to

$$\delta=\delta_{SV}\gamma_{SV}/\gamma$$

where γ is so-called Hermann's function

$$\gamma\equiv\sin^{1/3}\varphi\Big/\left[4\int_0^{\varphi}\sin^{1/3}\varphi d\varphi\right]^{1/4}$$

and δ_{SV} is the value of δ at φ_{SV} and γ_{SV} the value of γ at φ_{SV}. Such a distribution of the vapor film thicknesses δ is considered to be one of arbitrary functions that become δ_{SV} at φ_{SV} and infinitely large at the rear stagnation point. δ may be chosen identically set equal to δ_{SV} or infinity in the region from φ_{SV} to π. Of course, it is not guaranteed that the temperature distribution in the vapor film is a linear function of y beyond φ_{SV} as in the upstream region up to φ_{SV}. Such approximate treatment might be allowed because the influence of heat transfer in the downstream region of φ_{SV} on the average heat transfer for an entire cylinder is small.

For water, since Δt is larger than $\Delta\ell$ near the forward stagnation point, the above mentioned procedure can not be applied. Therefore, a different calculation scheme was prepared for water (the description of it is omitted here). Numerical integration was thus performed until $\Delta\ell$ became equal to Δt. Thereafter the above mentioned scheme for $\Delta\ell>\Delta t$ was applied.

liquid	$K\equiv\frac{\rho_L}{\rho_V}$	$R\equiv\left(\frac{\rho_V\mu_V}{\rho_L\mu_L}\right)^{1/2}$	Pr_L	$B_L\equiv\frac{\beta_L\ell}{Cp_L}$	reduced pressure
water	1600	0.0051	1.76	0.417	0.00458
ethanol	476	0.0073	8.50	0.372	0.00334
hexane	200	0.014	4.27	0.214	0.0158

Table 1 Dimensionless parameters and reduced pressure

5. Results and Discussion

Numerical calculations were carried out for water, ethanol and hexane under the standard atmospheric pressure (1.013 bar). Density ratio K, $\rho\mu$ ratio R, Prandtl number of liquid Pr_L, buoyant force parameter B_L and the reduced pressure corresponding to the atmospheric pressure for these liquids are listed in Table 1. The ranges of calculations for Froude number Fr, dimensionless superheating Sp and dimensionless subcooling Sc are as follows

$Fr = 0.0005 \sim 500$

water : $Sp=0.5 \sim 2.0$, $Sc=0 \sim 0.1$

ethanol : $Sp=0.5 \sim 2.0$, $Sc=0 \sim 0.045$

hexane : $Sp=1.0 \sim 2.5$, $Sc=0 \sim 0.12$

The result of calculation for ethanol is presented below in greater detail as a typical result because water, which represented liquids dealt with in the first report, has the characteristics different from those of the other two liquids concerning the ratio of the two liquid boundary-layer thicknesses, as stated above.

5.1 Velocity profile, separation point and ratio of vapor film thickness to liquid thermal boundary-layer thickness

The velocity profiles for ethanol are shown in Fig.2, in which the ratio of the velocity in the vapor film u_V to the velocity at the vapor-liquid interface u_δ and the ratio of the velocity in the liquid u_L to u_δ at the stagnation point ($\varphi=0$) are taken as the ordinate and y/δ and $\zeta/\Delta\ell$ as the abscissa. The region where the body force predominates is represented by the result for $Fr=0.005$ ($\sqrt{Fr}=0.071$), the region where the effects of body force and forced convection are comparable by that for $Fr=0.25$ ($\sqrt{Fr}=0.5$), and the region where the forced convection predominates by that for $Fr=50$ ($\sqrt{Fr}=7.1$). The description of the predominant forces in this context is consistent with those

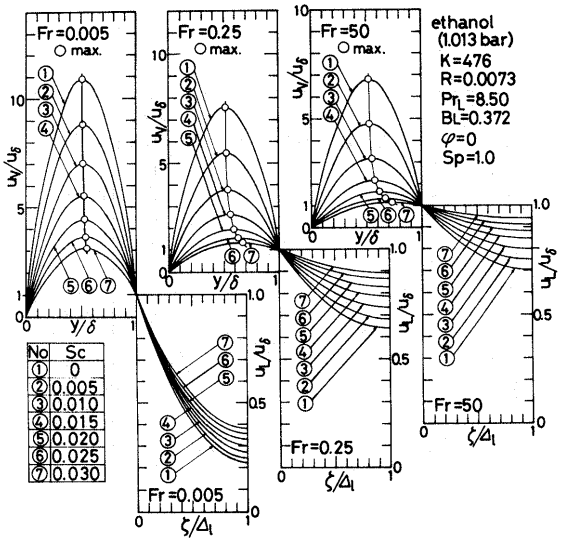

Fig.2 Velocity profile

in the first report for a saturated liquid. The division of the region by predominant forces for a subcooled liquid will be described later after introducing Fig.5.

In Fig.2, as dimensionless subcooling Sc is increased,

(i) the maximum of the ordinate u_V/u_δ in the vapor film becomes smaller and the position of the abscissa y/δ corresponding to the maximum moves to the vapor-liquid interface ($y/\delta=1$);

(ii) the value of u_L/u_δ in the liquid boundary-layer approaches unity (this means that the velocity u_δ becomes smaller and the velocity in the liquid becomes smaller throughout the boundary-layer and the resulting velocity profile gets flat because the velocity of the free stream is held constant if Fr is fixed.); and

(iii) the relations described in (i) and (ii) are remarkably observed for large Fr.

In the case of large approaching velocity of liquid and large degree of subcooling, the velocity profile in the vapor film becomes a parabola having small maximum and the velocities u_δ and u_L approach that of the free stream (a potential flow). This is caused by the fact that the vapor film becomes thinner with an increase in the degree of subcooling and the vapor is unlikely to accelerate because the viscous shear stress due to the existence of a solid wall (a heating wall) governs the flow in the vapor film and the pressure gradient transmitted from the free stream becomes less effective.

The vapor flow separates if Fr is larger than 1/8 as it was the case with a saturated liquid. However, in this case of a subcooled liquid, as already mentioned in Section 4, something occurs before the separation. The velocity at the vapor-liquid interface becomes equal to that of the free stream and the velocity in the liquid has a flat profile at a certain angular position φ_{SL} before the vapor flow separates. Thus, we have assumed that the velocity in liquid u_L is equal to that of the potential flow ($\equiv 2f^{1/2}\sin\varphi$) everywhere downstream of the point φ_{SL}. By this assumption, the condition of separation $(\partial u_V/\partial y)_0=0$ reduces to

$$\varphi=\varphi_{SV}:\quad 4\sqrt{2}F_r^{1/2}\sin\varphi+\delta^2K\sin\varphi(1+8F_r\cos\varphi)=0\ . \qquad \cdots\cdots(31)$$

Separation point φ_{SV} determined by Eq.(31) is shown by fine solid curve for ethanol in Fig.3. In this connection the separation point φ_S for a saturated liquid is able to be expressed approximately as $\varphi_S=\cos^{-1}(-1/8Fr)$ (shown by bold solid curve in Fig.3). It is seen from Fig.3 that φ_{SV} becomes larger with an increase of Sc, the limiting value for small subcooling being φ_S. That is, the separation is delayed when the liquid is subcooled. The predominance of the effect of the shear stress over that of the pressure gradient transmitted from the free stream makes the second term of l.h.s. in Eq.(31) less effective with an increase of liquid subcooling. For all Sp chosen it is found that the difference between φ_{SV} and φ_S reduces with an increase of Sp.

The angular variation of the ratio of liquid thermal boundary-layer thickness to vapor film thickness ($\Delta t/\delta$) is shown in Fig.4(a). The ratio ($\Delta t/\delta$) is nearly constant except near the separation point φ_{SV} (shown by symbol ○) and the ratio ($\Delta t/\delta$) is constant in a wider range of φ as the degree of subcooling is increased. This is clearly seen from the following equation (32), which is obtained by substituting Eq.(21) into the energy equation for the vapor film, Eq.(13) with the evap-

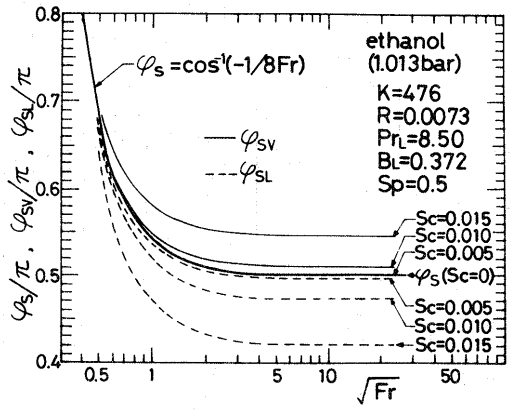

Fig.3 The relation among φ_{SL}, separation point φ_{SV}, dimensionless subcooling Sc and Froude number Fr

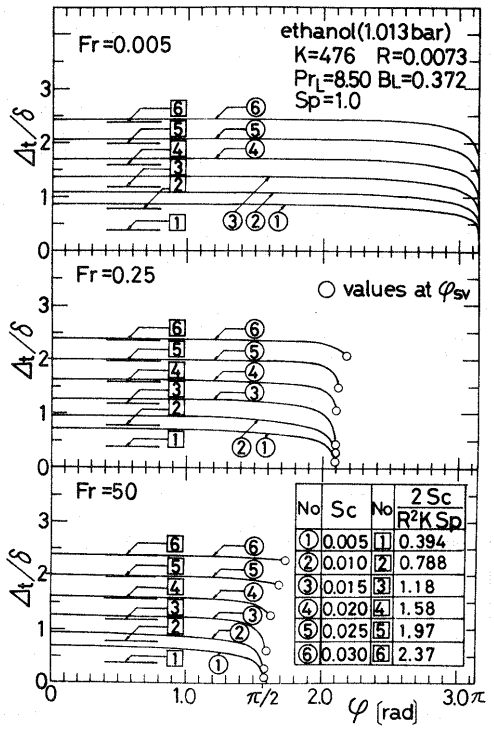

Fig.4(a) Angular distribution of the ratios of liquid thermal boundary-layer Δt to vapor film thickness δ

oration term in l.h.s. discarded. The omission of that contribution may be inferred from the suppressed rate of evaporation in a subcooled liquid.

$$\Delta_t/\delta=(2/R^2K)(S_c/S_p) \quad \cdots\cdots(32)$$

Therefore, it is expected from the above equation that the ratio $(\Delta t/\delta)$ will be independent of φ in the case of extremely large subcooling. The value of r.h.s. in this equation is indicated by horizontal line segments in the figure. The ratio $(\Delta t/\delta)$ at the forward stagnation point is shown against Sc in Fig.4(b). In the figure, the ordinate $(\Delta t/\delta)_{\varphi=0}$ approaches the curve given by Eq.(32) irrespective of Fr and Sp.

5.2 Heat transfer

Figure 5 shows the dependence of $(Nu_D/\sqrt{Re_L})(\mu_V/\mu_L)$ (hereafter this quantity is designated as ϕ) on Froude number Fr for ethanol with dimensionless subcooling Sc as the parameter. The relation between ϕ and the approaching velocity in the regions of small Fr and of large Fr is similar to that for a saturated liquid and the region where the dependence of ϕ on Fr turns somewhat abnormal gets narrower with an increase of the degree of subcooling. The existence of the abnormal region just mentioned is the result of a movement of the separation point with respect to Fr . This was discussed in the first report in detail. In Fig.5, the ordinate ϕ decreases continuously from the small Fr region where the body force predominates, to the large Fr region where the forced convection predominates, and the two regions are approximately divided around $Fr=0.25$ $(\sqrt{Fr}=0.5)$. Therefore it is conjectured that the effect of separation on heat transfer lessens with an increased subcooling due to the delayed separation as shown in Fig.3. The comparison between $Sp=0.5$ and $Sp=1.0$ in Fig.5 indicates that the effect of subcooling is more remarkable for smaller superheating and larger Fr, i.e., larger approaching velocity.

The dependence of ϕ on Sp for fixed Sc , ϕ seems proportional to $Sp^{-1/4}$ for a saturated liquid and proportional to Sp^{-1} for a strongly subcooled liquid. From these considerations, in the case of large subcooling, ϕ_{NSUB} has been chosen as the dimensionless parameter for heat transfer in the region of predominant body force and ϕ_{FSUB} in the region of predominant forced convection. They are defined by

$$\phi_{NSUB}\equiv(N_{uD}/\sqrt{R_{eL}})(\mu_V/\mu_L)(F_r/B_LS_c)^{1/4}\times(S_p/S_c)(1/P_{rL})^{1/2} \quad \cdots\cdots(33)$$

$$\phi_{FSUB}\equiv(N_{uD}/\sqrt{R_{eL}})(\mu_V/\mu_L)(S_p/S_c)(1/P_{rL})^{1/2}. \quad \cdots\cdots(34)$$

These expressions of ϕ_{NSUB} and ϕ_{FSUB} are derived by applying heat tansfer correlation for single-phase laminar flow ($Nu_D\propto(Gr_DPr_L)^{1/4}$ for natural convection, $Nu_D\propto(Re_LPr_L)^{1/2}$ for forced convection) to Δt in Eq.(32). In the case of a saturated liquid in the first report, numerical results were reduced by utilizing ϕ_{NSAT} (ϕ_N in the first report) for the region of predominant body force, and ϕ_{FSAT} (ϕ_F in the first report) for that of predominant forced convection respectively. They were defined by

$$\phi_{NSAT}\equiv(N_{uD}/\sqrt{R_{eL}})(\mu_V/\mu_L)(F_rS_p/R^4K)^{1/4} \quad \cdots\cdots(35)$$

$$\phi_{FSAT}\equiv(N_{uD}/\sqrt{R_{eL}})(\mu_V/\mu_L)(S_p/R^4K)^{1/4}. \quad \cdots\cdots(36)$$

Heat transfer results for water (a) , ethanol (b) and hexane (c) are summarized against $Fr=0.005$ 0.25 and 50 in Fig.6 using ϕ_{NSAT} , ϕ_{NSUB} , ϕ_{FSAT} and ϕ_{FSUB} .

5.3 Comparison with experimental data

Figures 7(a) and 7(b) show a comparison between the present analysis and the experimental data of ethanol by Motte-

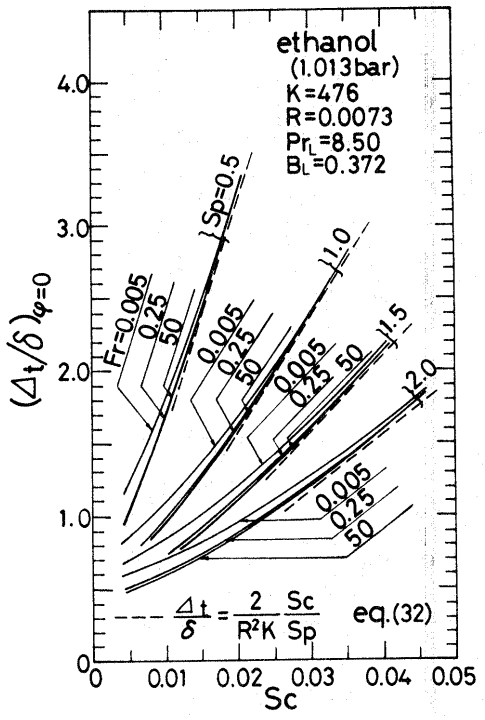

Fig.4(b) The relation among the ratio $(\Delta t/\delta)$ at the stagnation point, dimensionless superheating Sp, dimensionless subcooling Sc and Froude number Fr

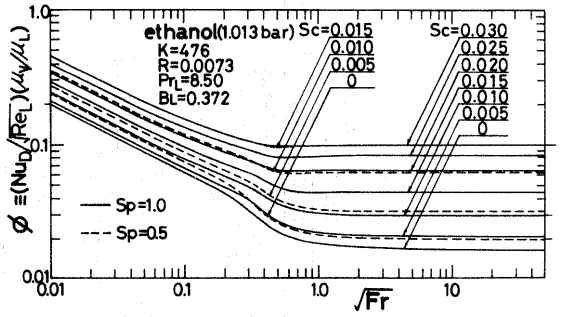

Fig.5 The relation among average Nusselt number $(Nu_D/\sqrt{Re})(\mu_V/\mu_L)$, dimensionless subcooling Sc and Froude number Fr

Bromley[2] and those of water by the present authors[4] respectively. Both experiments were conducted at the nominal atmospheric pressure and the diameters of the cylinder were 9.83 mm in the former and 16 mm in the latter. The present analysis is indicated by solid curve and the approaching velocity U_∞ and the degree of subcooling ΔT_{sub} are given in the figures. The average heat transfer coefficient α_D obtained by experiment is two or three times as high as that by the present analysis. In Fig.7, the value given by the semi-theoretical correlation (Eq.(45) in Reference (3)) for a sphere and a cylinder by Epstein-Hauser[3] is also indicated by dotted curve.

6. Conclusions

Forced convection film boiling heat transfer from a horizontal cylinder to a subcooled liquid cross-flowing upward was analysed based on the two-phase boundary-layer theory by means of the integral method of boundary-layer. Numerical solutions were determined for water, ethanol and hexane under the atmospheric pressure. The fundamental characteristics of film boiling heat transfer in external-flow field were clarified. Locating the cause of the discrepancy between the experimental data and the analysis and the proposition of heat transfer correlation are open to future studies.

The authors wish to thank Prof. Nakashima of Nagasaki University who offered them various conveniences. One of the authors, T.Shigechi, was awarded a scholarship from the Japan Society for the Promotion of Science as a visiting researcher at Kyushu University in the fiscal 1980 and this study was financed partially by the Grant-in-aid for Scientific Research, General Research B [446088] of the Japanese Ministry of Education, Science and Culture. Numerical calculations were carried out on FACOM M-200 PPS in Computer Center of Kyushu University.

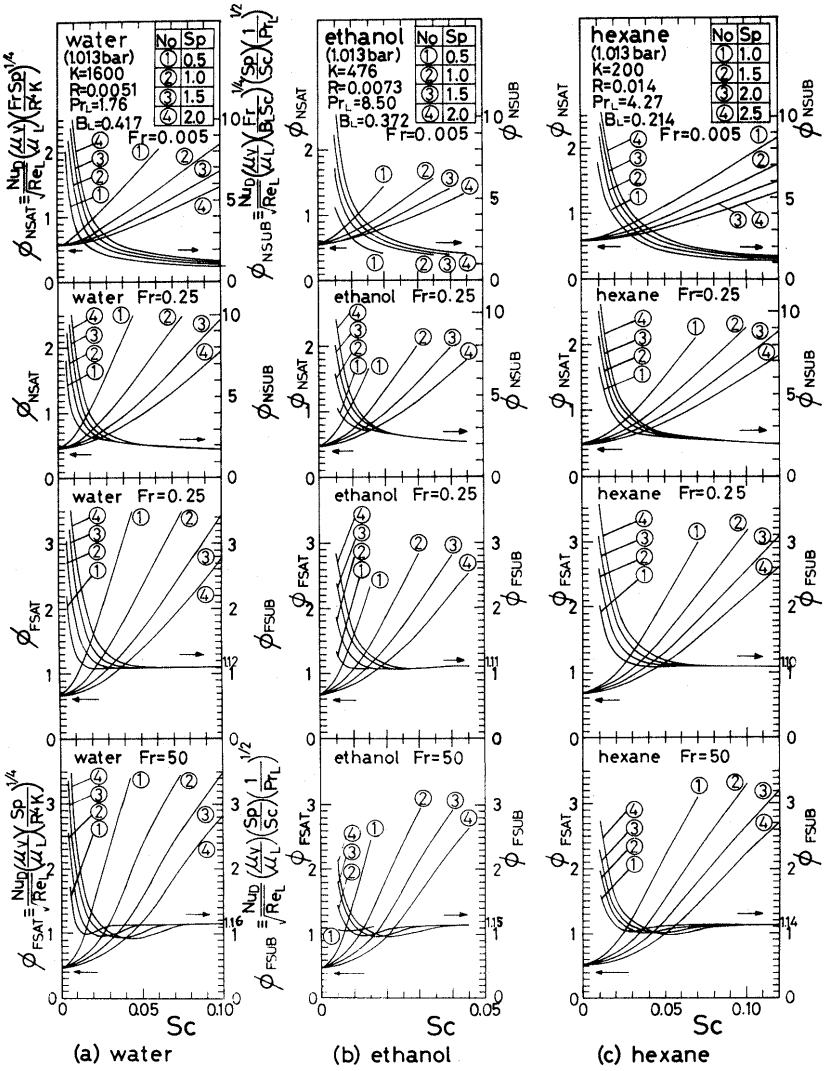

Fig.6 Heat transfer results

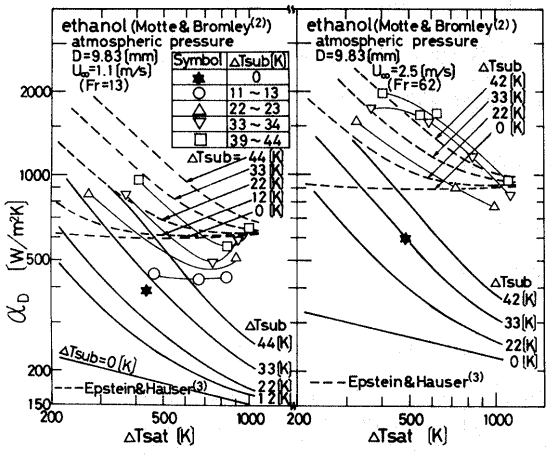

Fig.7(a) The comparison of the present analysis with the experimental data for ethanol by Motte-Bromley

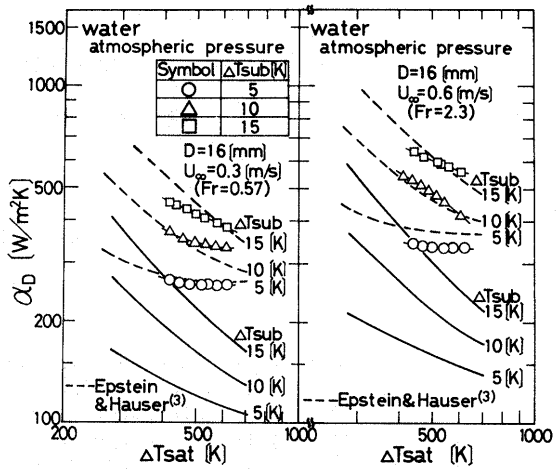

Fig.7(b) The comparison of the present analysis with the experimental data for water by the authors

References

(1) Ito, T., et al., Bull. JSME, Vol.24, No.198 (1981), p.2107.
(2) Motte, E.I. & Bromley, L.A., Indust. & Engng. Chem., Vol.49, No.11 (1957), p.1921.
(3) Epstein, M. & Hauser, G.M., Int. J. Heat & Mass Transf., Vol.23, No.2 (1980), p.179.
(4) Nishikawa, K., et al., 15th National Heat Transfer Symposium of Japan (in Japanese) (1978), p.193.